Recognizing Continuous Multiple Degrees of Freedom Foot Movements With Inertial Sensors

Chenyao Zhu, *Student Member, IEEE*, Lan Luo, Jingeng Mai, and Qining Wang, *Senior Member, IEEE*

***Abstract*— Recognition of continuous foot motions is important in robot-assisted lower limb rehabilitation, especially in prosthesis and exoskeleton design. For instance, perceiving foot motion is essential feedback for the robot controller. However, few studies have focused on perceiving multiple-degree of freedom (DOF) foot movements. This paper proposes a novel human-machine interaction (HMI) recognition wearable system for continuous multiple-DOF ankle-foot movements. The proposed system uses solely kinematic signals from inertial measurement units and multiclass support vector machines by creating error-correcting output codes. We conducted a study with multiple participants to validate the performance of the system using two strategies, a general model and a subject-specific model. The experimental results demonstrated satisfactory performance. The subject-specific approach achieved 98.45% ± 1.17% (mean ± SD) overall accuracy within a prediction time of 10.9 ms ± 1.7 ms, and the general approach achieved 85.3% ± 7.89% overall accuracy within a prediction time of 14.1 ms ± 4.5 ms. The results prove that the proposed system can more effectively recognize multiple continuous DOF foot movements than existing strategies. It can be applied to ankle-foot rehabilitation and fills the HMI high-level control demand for multiple-DOF wearable lower-limb robotics.**

***Index Terms*— Foot movement, continuous recognition, inertia sensors, wearable robotics.**

Manuscript received May 6, 2021; revised November 14, 2021 and January 24, 2022; accepted February 4, 2022. Date of publication February 7, 2022; date of current version February 25, 2022. This work was supported in part by the National Key Research and Development Program of China under Grant 2018YFB1307300 and Grant 2018YFE0114700; in part by the National Natural Science Foundation of China under Grant 91948302, Grant 51922015, and Grant 52005011; and in part by the PKU-Baidu Fund under Grant 2020BD008. *(Corresponding author: Qining Wang.)*

This work involved human subjects or animals in its research. Approval of all ethical and experimental procedures and protocols was granted by the Local Ethics Committee of Peking University, China.

Chenyao Zhu and Jingeng Mai are with the Department of Advanced Manufacturing and Robotics, College of Engineering, Peking University, Beijing 100871, China, and also with the Beijing Engineering Research Center of Intelligent Rehabilitation Engineering, Peking University, Beijing 100871, China.

Lan Luo is with the Department of Neurology, Beth Israel Deaconess Medical Center, Harvard Medical School, Boston, MA 22215 USA.

Qining Wang is with the Department of Advanced Manufacturing and Robotics, College of Engineering, Peking University, Beijing 100871, China, also with the Medical Robotics Laboratory, University of Health and Rehabilitation Sciences, Qingdao 266071, China, also with the Beijing Institute for General Artificial Intelligence, Beijing 100080, China, and also with the Institute for Artificial Intelligence, Peking University, Beijing 100871, China (e-mail: qiningwang@pku.edu.cn).

Digital Object Identifier 10.1109/TNSRE.2022.3149793

I. Introduction

OVER the past few decades, researchers have made great efforts to design and implement robot-assisted lower-limb devices such as anthropomorphic exoskeletons and prostheses to enhance or recover human capabilities. Compared with the many developments in the mechanical configuration and hardware-level controller, challenges still exist in human-machine interaction (HMI) at the high level of the control hierarchy. One crucial problem that needs to be given more attention is quickly perceiving the user's motion intention to coordinate with the device relatively efficiently and safely [1].

In particular, perceiving ankle-foot motions is one challenge of HMI high-level control in robot-assisted lower limbs. A human foot can supply multiple DOFs to provide flexibility in foot movements. Meanwhile, a human central control system regulates ambulation. Sensory control from the spine and brain makes a human respond quickly to maintain balance during locomotion, including perceiving, adjusting, and reacting to the environment. Unlike the movements of a human foot, existing anthropomorphic exoskeletons and bionic robots lack the flexibility for fine motor control and, therefore, cannot imitate human foot movement [2]–[6]. Since HMI serves an essential tool for humans to control machines through natural and intuitive behaviors [7], [8], we expected some wearable lower-limb robotics with an HMI system. The system could quickly perceive the user's foot movement intent to achieve the goal so that wearable robotics can fit the user and work more in concert with the user's movements.

Recent user mode recognition of wearable lower-limb robots has mainly focused on terrain or gait pattern recognition [1], [9]–[14]. To adapt to the natural movements of a human body, it is vital to design wearable robots in terms of the range of motion and the DOFs accompanied by continuous locomotion. Unfortunately, current wearable lower-limb robotics mostly provide a single DOF for the foot. Only a few can provide two DOFs for the foot. Although the Berkeley Lower Extremity Exoskeleton (BLEEX) featuring three DOFs at the ankle, only one DOF, the ankle plantar/dorsiflexion, is actuated [15], [16]. Furthermore, there is limited human motion mode recognition research on continuous foot gestures or multiaxial foot movements [1], [17]–[19]. Scott *et al.* designed a study performing foot gesture recognition involving 2-DOF foot movement under static conditions [19]. Gregory and Ren tried different strategies to recognize continuous multiaxial ankle-foot motions based on surface electromyography (sEMG) data. The motions to be predicted were in two DOFs, the sagittal plane (foot

dorsiflexion and plantarflexion), and the frontal plane (foot eversion and inversion) [17].

Moreover, in robot-assisted mode, users wear exoskeletons on the existing limbs compared to prostheses. Exoskeletons must work in concert with the user's intrinsic limb movements. In particular, orthoses are a unique exoskeleton device to assist individuals suffering from limb pathology and work consistent coordination [20], making the movement recognition HMI control strategy more important. However, current research has developed only a paucity of recognition HMI control strategies for exoskeletons but for prosthetic devices. Primarily, there are limited studies about mode recognition HMI of ankle-foot orthoses (AFOs) [1], [21]–[35]. Thus, there is a compelling need to design a mode recognition for HMI high-level control wearable systems into AFOs to improve patient engagement during physical therapy. Hence, in pursuing an imitation that approaches the natural functions of a human foot and to develop HMI with intuitive feedback control for wearable lower limb robotics, especially for AFOs, this paper proposed an HMI wearable system to recognize multiple DOFs of fine ankle-foot movements during a continuous locomotion mode. We designed this study to improve a user's experience with ankle-foot rehabilitation in the future.

We organized the rest of this paper as follows: Section II-A gives a brief description of natural human foot movements to introduce the recognition target motion definitions in this study. After describing the system design (Section II-B) and how we conducted the experiments (Section II-C), Section II-D illustrates the algorithm protocol, including two distinct recognized model-designed strategies. We presented the experimental results in Section III and discussed them in Section IV. Finally, a conclusion is provided in Section V.

II. Methods

A. Target Motions Definition

In this paper, we described and defined the foot's movements according to the anatomical position and anatomical plane (Fig. 1(a)). The anatomical position is the point of reference for all movements.

Normal walking consists of plantarflexion and dorsiflexion of the foot occurring in the sagittal plane to generate successful forward bipedal locomotion (Fig. 1(a, b)). A human foot can supply other DOFs for more flexibility of foot movements than most other mammals. Eversion of the foot moves it away from the midline, while inversion moves it toward the midline (Fig. 1(c)). The foot subtalar joint formed between the talus and calcaneus controls both inversion and eversion, which occur in the frontal plane (Fig. 1(a)). Abduction moves the foot laterally away from the body's midline, while adduction is the opposite action (Fig. 1(d)). These are movements in the transverse plane [36], Fig. 1(a). The ankle joint plays an important role in foot mechanics, and the tibia and fibula of the leg and talus of the foot form the ankle joint, which plays a vital role in foot mechanics.

B. System Description

Fig. 2 (the system configuration) and Fig. 3 (the system layout) show our sensor design, a fully portable and wearable wireless system for measuring plantar pressure and foot dynamics data. The system has all logic elements required for monitoring continuous dynamics signals in real-time (Fig. 2(d)) based on the force and inertial sensor readings onboard. The system consists of two sensing insole units, four inertial measurement units, and a control box unit designed by our team. To ensure that the sensor was in the correct position for each subject during each trial, we utilized footwear to locate the sensor units with two configurations available (one for female Fig. 2(a) and the other for males Fig. 2(b)). Our system is convenient to carry and wear and a user can don it in less than two minutes.

Each sensing insole unit consists of a multicell piezoresistive sensor and a logic unit. The customized multicell insole features sixteen piezoresistive sensors that capture most of the area of the plantar forces (Fig. 2(c)). An ADC amplifies and

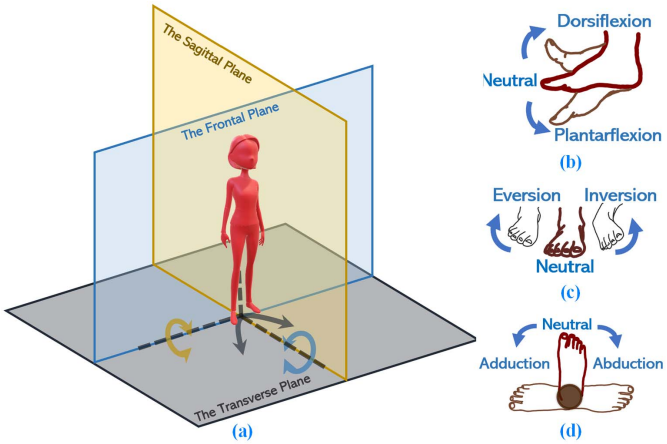

The Sagittal Plane	Dorsiflexion-Plantarflexion Occurs
The Frontal Plane	Inversion-Eversion Occurs
The Transverse Plane	Abduction-Adduction Occurs

Fig. 1. (a) The anatomical plane used in this study and (b-d) the foot movements defined in the study.

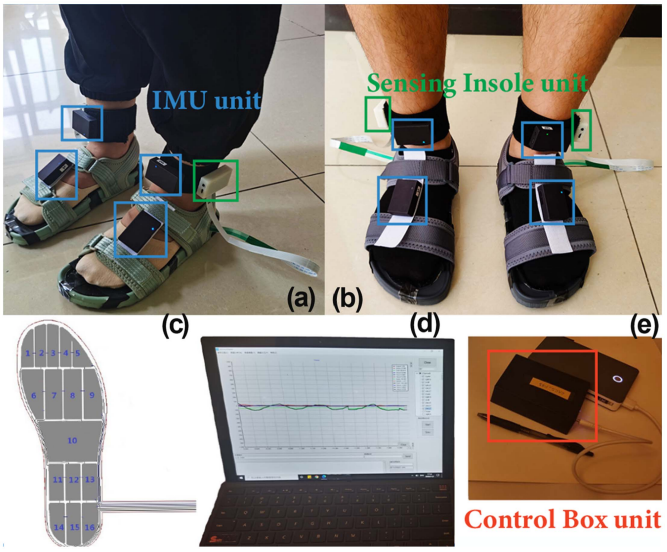

Fig. 2. (a) A female subject wearing the system. (b) A male subject wearing the system. (c) Customized multicell insole, (d) real-time monitoring, and (e) power bank powering the control box.

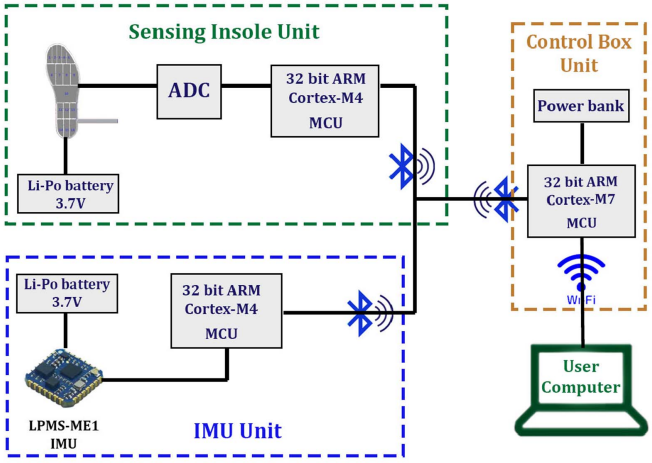

Fig. 3. System layout.

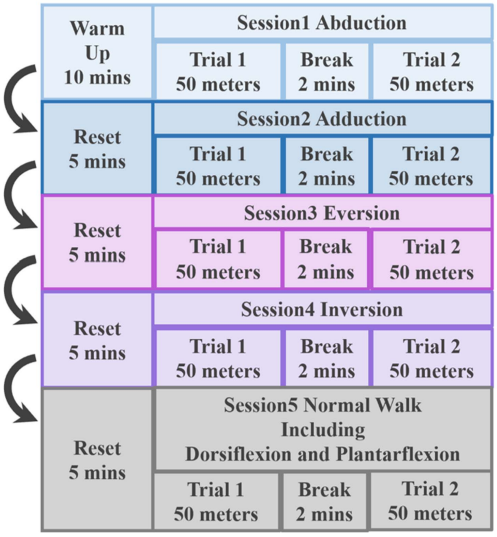

Fig. 4. Experimental protocol.

digitizes the signals and then feeds the signals to a 32-bit ARM Cortex-M4 Processor in the logic unit. The inertial measurement unit (IMU) has 9-DOF. The IMU units are located along the midline of the foot, one placed above the center of the lateral cuneiform and the intermediate cuneiform, and the other tied above the talus and the bottom of the tibia.

A 3.7 V Li-Po battery independently powers all sensor units. The sensing units collect signals at 100 Hz and wirelessly sends them to a power-bank powered control box via Bluetooth® technology (Fig. 2(e)). The control box contains a 32-bit ARM Cortex-M7 Processor, synchronizing the sensing units'signals and sending them to the user computer over a WLAN using a Wi-Fi module. The user can wear the control box unit or locate it within a 50 m range from the user.

C. Experimental Protocol

The Local Ethics Committee of Peking University approved the protocol for this study, and all subjects provided informed consent before the experimental session.

1) Participants: Data were collected from seven healthy adult individuals with no musculoskeletal or neurological conditions. Four females and three males (mean height 1.69 m, range 1.62-1.83 m; mean weight 63.1 kg, range 52-81 kg) were included.

2) Procedures: Subjects, based on sex, chose the corresponding system configuration as we described in the previous section (Fig. 2(a, b)).

Fig. 4 shows the protocol of the experiment. We instructed each volunteer and showed examples of what they should do in each foot session by demonstration. Then, we allowed the subject to exercise and familiarize each foot movement session under the instructor's supervision before starting the experiment. It is assumed the volunteers'feet have three-dimensional coordinate axes, as shown in Fig. 1. In Session 1, abduction: for each step, the foot rotates around the vertical-axis and laterally away from the body's midline during movement. Session 2, adduction: for each step, the foot rotates around the vertical axis and laterally toward the body's midline during locomotion. Session 3, eversion movement: for each step, the sole tilts outwards, rotating around the sagittal axis, and away from the body's midline. Session 4, inversion: the sole tilts toward the body's midline, rotating around the sagittal axis during movement. After the familiarization sessions, participants conducted five different mode sessions: abduction, adduction, eversion, inversion, and normal walking, including dorsiflexion and plantarflexion. Each mode type session included one trial with two-minute breaks and then another trial. Furthermore, the participant rested for 5 minutes between sessions to avoid fatigue. Each trial started with a six-second calibration, and subjects walked along a 50 m straight-line path at a self-selected, comfortable pace.

(a) Passage for trails (b) Eversion Session for Subject 3

Fig. 5. (a) The experimental environment; (b) Recording an ongoing trial.

As shown in Fig. 5, each trial was labeled by the instructor based on video references. Foot dynamics captured from both IMUs and pressure insoles were continuously monitored during the trial by our wireless real-time interactive system (Fig. 2(d)). To ensure a complete experiment, the technician could interrupt and restart the trial if anything went awry.

D. Algorithm Protocol

Fig 6 shows the flowchart of the model design strategy.

1) Preprocessing: The 100 Hz raw signals from the sensors were fed to our custom preprocessing algorithm. First, the

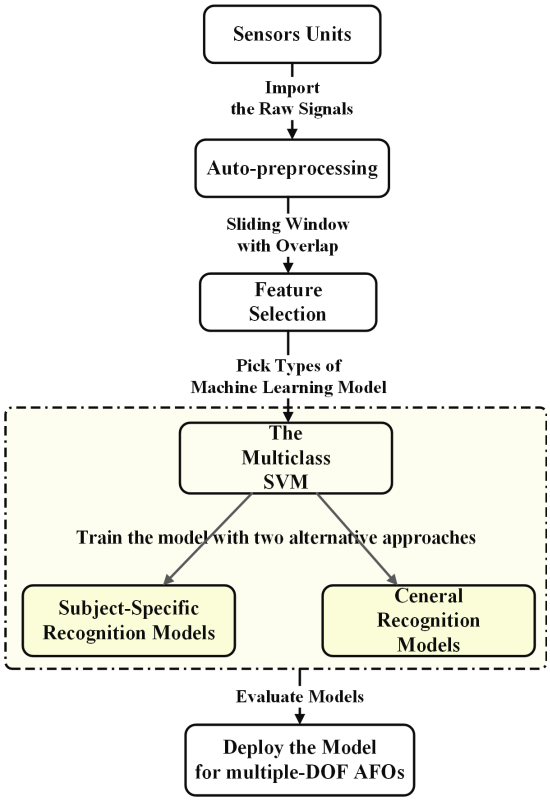

Fig. 6. Flowchart of the recognition model design.

algorithm picked up the working channels from the raw signals. Then, a 0.1-second sliding window was used to continuously detect and replace the outliers in the working channels of the data. A Gaussian filter was applied to reduce noise, and the continuous quadratic trend in the signals from the IMU sensors caused by drift was removed. Finally, the signals were normalized.

After preprocessing, the signals were split into two sets, one for stride segmenting and the division of dorsiflexion and plantarflexion based on the plantar force captured from the sensing insole and another for foot movement mode recognition using the foot dynamic signals from the inertial sensors. The mathematical model is presented in (1) and (2).

$$\begin{cases} \boldsymbol{Force}_i^{Leftfoot} = \left[\boldsymbol{F}_i^1, \boldsymbol{F}_i^2, \boldsymbol{F}_i^3, \ldots, \boldsymbol{F}_i^j \right] \\ \boldsymbol{Force}_i^{Rightfoot} = \left[\boldsymbol{F}_i^1, \boldsymbol{F}_i^2, \boldsymbol{F}_i^3, \ldots, \boldsymbol{F}_i^j \right] \\ i, j \in \mathbb{N};\ i = 0, 1, 2, 3, \ldots, n,\ n = datapoints \end{cases} \quad (1)$$

$$\begin{cases} \boldsymbol{X}_{IMU}^{LeftCuneiform} = \left[\boldsymbol{x}_i^{1(Yaw)}, \boldsymbol{x}_i^{2(Pitch)}, \boldsymbol{x}_i^3, \ldots, \boldsymbol{x}_i^j \right] \\ \boldsymbol{X}_{IMU}^{LeftTalusTibia} = \left[\boldsymbol{x}_i^{1(Yaw)}, \boldsymbol{x}_i^{2(Pitch)}, \boldsymbol{x}_i^3, \ldots, \boldsymbol{x}_i^j \right] \\ \boldsymbol{X}_{IMU}^{RightCuneiform} = \left[\boldsymbol{x}_i^{1(Yaw)}, \boldsymbol{x}_i^{2(Pitch)}, \boldsymbol{x}_i^3, \ldots, \boldsymbol{x}_i^j \right] \\ \boldsymbol{X}_{IMU}^{RightTalusTibia} = \left[\boldsymbol{x}_i^{1(Yaw)}, \boldsymbol{x}_i^{2(Pitch)}, \boldsymbol{x}_i^3, \ldots, \boldsymbol{x}_i^j \right] \\ i, j \in \mathbb{N};\ i = 0, 1, 2, 3, \ldots, n,\ n = datapoints \end{cases} \quad (2)$$

where $\boldsymbol{i}$ is the current data point and n is the number of data points within the signals. $\boldsymbol{F}_i^j$ of each matrix of plantar force is a column of the data points corresponding to the **j**-th piezoresistive sensor of the multicell sensing insole. $\mathbf{x}_i^j$ of each IMU matrix corresponds to the **j**-th particular dynamics signal, such as, $\boldsymbol{x}_i^{1(Yaw)}$, which is a column of data points for the yaw angle signal.

2) Feature Selection: Based on our preliminary experiments, the preprocessed IMU signals were better using a 75% overlap 1.2-second sliding window. Each x_i^j in (2) was converted into an N-by-120 matrix $\mathbf{x}_{N\times 120}^j$ representing N samples, and each sample contained 120 data points representing a 1.2-second time duration of kinematic signal information, such as,

$$\boldsymbol{x}_i^{1(Yaw)} \xrightarrow{Sliding\ \ Window} \mathbf{x}_{N\times 120}^{1(Yaw)},$$

where $N = samples$. We tried many features, such as the difference and mean absolute values (MAVs) [12], [17], and five time-domain features were chosen for minimal computational cost and memory consumption to be calculated from each sample of IMU signals. The features are defined as follows:

$$\begin{cases} \boldsymbol{feature1} = mean(\mathbf{x}) \\ \boldsymbol{feature2} = std(\mathbf{x}) \\ \boldsymbol{feature3} = maximum(\mathbf{x}) \\ \boldsymbol{feature4} = minimum(\mathbf{x}) \\ \boldsymbol{feature5} = mean(difference(\mathbf{x})) \end{cases} \quad (3)$$

where $\mathbf{x}$ stands for $\mathbf{x}_{N\times 120}^j$. The arithmetic mean measures the central tendency of the dynamic signals. The standard deviation is used to measure the spread of the dynamic signals. The maximum, minimum, and difference find the peaks in the continuous dynamics signals.

3) Movements Mode Recognition: We customize a multiclass support vector machine (SVM) by creating an error-correcting output code (ECOC) model for continuous foot movement recognition [37], [38]. The ECOC method streamlines the model to multiple binary SVMs using a one-vs.-one design. Then, the combination of the resulting classifiers is used for recognition. The idea is to design a robust construction consisting of several nonlinear separating hyperplanes for a quick and accurate response. The mathematical algorithm model is presented below:

After the feature selection procedure, we have a $N \times p$ size matrix for each IMU unit $\cdots\cdots$ (2). N represents the samples, while $\boldsymbol{p}$ represents the featured variables in each IMU matrix.

$$\mathbf{X}_{IMU} = \begin{pmatrix} \boldsymbol{x}^{1(Yaw\ \ featured1)_1} & \cdots & \boldsymbol{x}_1^p \\ \vdots & \ddots & \vdots \\ \boldsymbol{x}^{1(Yaw\ \ featured1)_N} & \cdots & \boldsymbol{x}_N^p \end{pmatrix}, \quad p, N \in \mathbb{N} \quad (4)$$

A nonlinear separating multidimensional hyperplane is defined by equation $f(x)$ for parameters β_0 and α_N by dividing multidimensional space into two halves using $\boldsymbol{p}$ features. One can easily determine on which side of the hyperplane a test observation lies by simply making use of both the magnitude and the sign of $f(x)$ $\cdots\cdots$ (5)

$$f(\boldsymbol{x}) = \beta_0 + \sum_{p\in S} \alpha_N K(\boldsymbol{x}, \boldsymbol{x}_N) \quad (5)$$

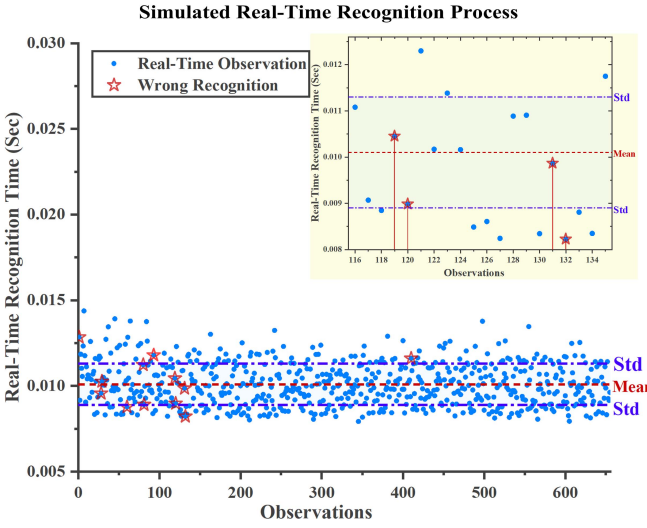

Fig. 7. Simulated real-time recognition processes. Each solid blue dot represents an observation. The red stars represent an error prediction of the corresponding observation. The purple dashed-dotted line represents the standard deviation of the prediction time for all observations in a real-time prediction trial. The red dashed line represents the average prediction time for all observations in a real-time prediction trial.

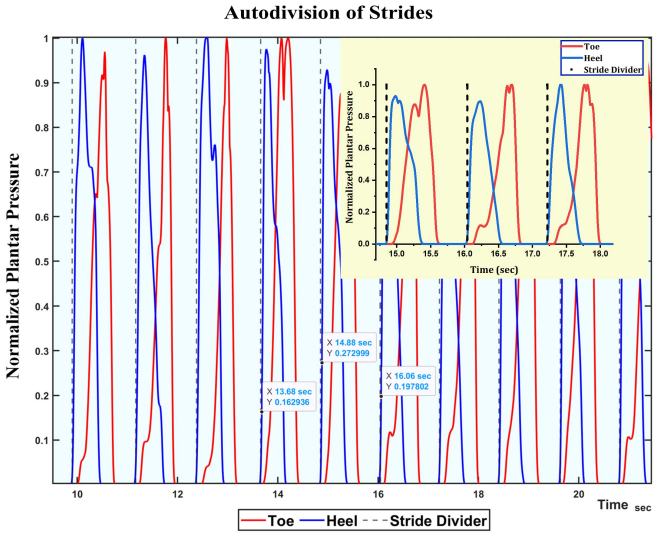

Fig. 8. Continuous autodivision of strides. The black dotted lines represent the beginning of a stride, and between two adjacent black dashed lines represent a gait cycle. The solid blue line represents the heel pressure after autosignal processing. The solid red line represents the toe pressure after autosignal processing.

$\boldsymbol{x}$ is an observation sample with the $\boldsymbol{p}$-featured variables. $K(x, x_N)$ is a polynomial kernel of degree $\mathbf{d}$, where $\mathbf{d}$ is a positive integer ····· (6)

$$K(\boldsymbol{x}, \boldsymbol{x}'_N) = (1 + \sum_{k=1}^{p} \boldsymbol{x}_{Nk} \boldsymbol{x}'_{Nk})^d \tag{6}$$

$\boldsymbol{S}$ is the collection of indices of the support points and defined by α_N being nonzero, which is the inner product of two observations x_N, x'_N given by

$$\langle \boldsymbol{x}, \boldsymbol{x}'_N \rangle = \sum_{k=1}^{p} \boldsymbol{x}_{Nk} \boldsymbol{x}'_{Nk} \neq 0 \tag{7}$$

We implemented two alternative recognition approaches as described below. Fig. 7 shows the process of simulated real-time recognition. *1) Subject-specific recognition approach:* This approach independently applied each subject's data set, which learns from the training data set of a specific subject and fits a set of coefficients of a recognition model tailored to that subject. We then selected the best learning model with the most negligible loss for that specific subject. Given each individual's data set had a small number of observations, to achieve the most reliable and accurate subject-specific models, we applied a tenfold cross-validation model assessment method to evaluate the subject-specific model [38], [41]. The tenfold cross-validation assessment method randomly divided the data set into ten subsets, nine subsets used for training, and the one remaining subset used for testing. The evaluation process used different training and test subsets each time, repeating the model evaluation process ten times. Finally, we evaluated the picked model recognition ability under simulated real-time conditions using a new data set for each subject.

2) General recognition approach: The general recognition model learned the fitted model for each subject based on the data sampled from all the subjects. Given the extensive data set of the general approach, we chose holdout validation [38], [41]. To achieve the most reliable and accurate model, we increased the randomness of the partition fraction based on multiple trials. We expanded the fraction range of the random data for validation to 10-30%. Thus, we applied the corresponding 90-70% random partition holdout validation on all subjects'data sets. That is, we used random 90-70% data sets for training and the other 10-30% data sets for testing. Then, we selected the best learning model with the most negligible loss for all subjects. Finally, we evaluated the trained model recognition ability under simulated real-time conditions by using a new data set for each subject.

III. Results

A. Signal Sources of the System Information

Our threshold-based method combined with plantar pressure signals from the customized multicell insole determined the gait cycle and labeled the foot movement modes. Fig. 8 shows the result of the continuous autodivision strides procedure for a random trial described in Section II-D. Note that our system can detect the contact of the toe and heel with the ground, thereby segmenting each stride successfully.

Fig. 9 and Fig. 10 show plots of the six-mode distribution curves of one side of a foot's normalized raw dynamic signals and the three-angle channels of the IMU units. We can see from Fig. 9 and Fig. 10 that except for dorsiflexion and plantarflexion, which look similar, the raw dynamic signals from each channel of the IMU unit vary in the most different foot movement modes. Both figures imply that the combination of the dynamic signals we chose was able to distinguish most of the different foot modes. However, we still need to ensure

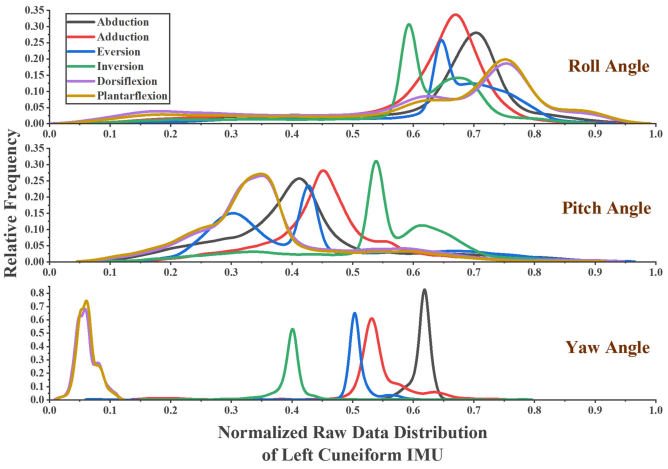

Fig. 9. The six-movement mode distribution curve of the total subject normalized raw dynamic signals. The three angle channels of the left foot cuneiform IMU unit are plotted.

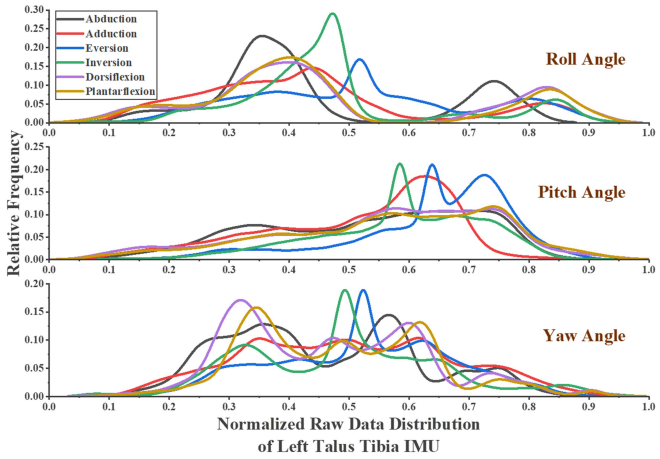

Fig. 10. The six-movement mode distribution curve of the total subject normalized raw dynamic signals. The three angle channels of the left foot talus tibia IMU unit are plotted.

efficient feature selection to distinguish the subtle differences of confusing modes in continuous locomotion for the model to produce accurate recognition results.

B. Validity and Reliability

Based on our experiment described in Sections II-C and II-D, Fig. 11 shows the overall recognition results for each subject using the two approaches. Table I shows the recognition confusion matrix, presenting the results of the mean and standard deviation across all subjects for six modes of continuous multiple-DOF foot movements under the two approaches. We performed two one-tailed (upper tail) t-tests with a 99% confidence level $((1-\alpha)\cdot 100\%, \alpha = 0.01)$ to test the statistical significance of the system recognition accuracy effects for two approaches separately. The one-tailed t-test is often used in hypothesis testing to determine whether an approach has an effect on our observing interests. A statistical t-test is relatively common in the statistical inference community. We test against the alternative hypothesis that the system's recognition accuracy

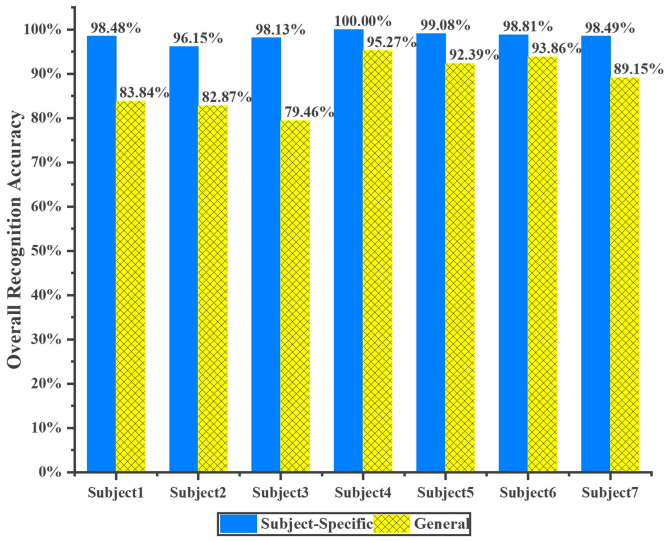

Fig. 11. Each subject's recognition overall accuracy results for the two model design strategies, the general approach, and the subject-specific approach.

steadily tends in one direction of effect greater than 1/2 [42], [43]. For the subject-specific approach, the total subject overall recognition accuracy in the three rotation DOFs along the three planes varied from 96.15 to 100% (98.45% ± 1.17%, mean, and SD) ($p < 0.0001$). For the general approach, total subject overall recognition in the three rotation DOFs along the three planes accuracy varied from 79.46 to 95.27% (85.3 ± 7.89%, mean, and SD) ($p < 0.0001$). The test statistic revealed that the system prediction accuracies have high statistical significance ($p < 0.0001$). In addition, before the t-test, to check the normality assumption of the t-test, we conducted the normality test for the null hypothesis that the recognition accuracy of either approach obeys normal distribution. Under the subject-specific approach, recognition accuracy accepts the null hypothesis ($p = 0.35$) and obeys normal distribution. Under the general approach, recognition accuracy also accepts the null hypothesis ($p = 0.47$) and obeys normal distribution. The results implied that both approaches with our system could effectively identify continuous multiple-DOF foot movements.

Fig. 12 shows each recognition mode summary statistic result from the distribution across all subjects by the two approaches. We also performed a two-tailed paired t-test with a 99% confidence level $((1-\alpha)\cdot 100\%, \alpha = 0.01)$ to test the statistical significance of the difference in recognition accuracy of our two approaches ($p = 0.0026$). The two-tailed t-test is often used in hypothesis testing to determine whether the interest groups of two approaches differ without specifying direction. The null hypothesis is that the recognition accuracy population of the two approaches comes from the same distribution [42], [43]. The test statistic found a highly statistically significant difference in the recognition accuracy of the two approaches ($p = 0.0026$).

C. Prediction Time

Table II shows the simulated real-time recognition time results of the two approaches of all strides across all subjects.

TABLE I
THE CONFUSION MATRIX OF THE RESULTS OF THE TOTAL SUBJECT FOOT MOVEMENTS DETECTION OF THE TWO APPROACHES (MEAN ± SD)

		Abduction	Adduction	Dorsiflexion	Eversion	Inversion	Plantarflexion
Subject-Specific	Abduction	99.77 0.39%	0.0 0.0%	0.0 0.0%	0.0 0.0%	0.0 0.0%	0.23 0.39%
	Adduction	0.0 0.0%	100.0 0.0%	0.0 0.0%	0.0 0.0%	0.0 0.0%	.0 0.0%
	Dorsiflexion	0.0 0.0%	0.0 0.0%	94.53 3.52%	0.0 0.0%	0.0 0.0%	5.47 3.52%
	Eversion	0.0 0.0%	0.0 0.0%	0.0 0.0%	100.0 0.0%	0.0 0.0%	0.0 0.0%
	Inversion	0.0 0.0%	0.0 0.0%	0.0 0.0%	0.0 0.0%	100.0 0.0%	0.0 0.0%
	Plantarflexion	0.0 0.0%	0.0 0.0%	6.81 7.22%	0.0 0.0%	0.0 0.0%	93.19 7.22%
General	Abduction	87.96 15.73%	5.30 13.19%	1.23 2.25%	4.65 12.31%	0.24 0.41%	0.61 1.45%
	Adduction	1.96 2.64%	84.76 20.36%	5.27 10.53%	0.42 0.6%	1.52 2.16%	5.07 11.5%
	Dorsiflexion	4.17 5.57%	3.54 7.1%	79.31 23.97%	0.22 0.58%	0.16 0.41%	12.61 14.39%
	Eversion	0.69 1.16%	0.13 0.35%	0.17 0.33%	93.64 7.27%	4.722 6.7%	0.63 0.99%
	Inversion	6.49 10.78%	4.36 4.58%	0.0 0.0%	0.63 1.12%	88.44 8.67%	0.08 0.22%
	Plantarflexion	5.04 8.27%	2.70 4.59%	1.32 2.56%	0.37 0.64%	0.0 0.0%	90.56 12.53%

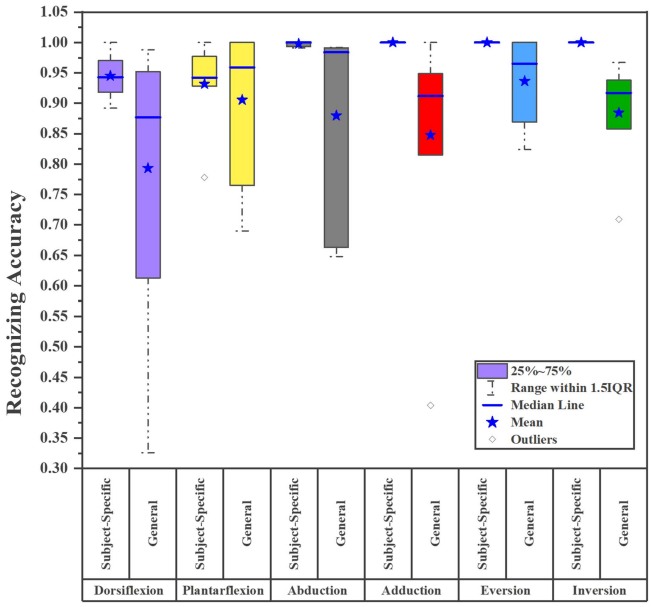

Fig. 12. Box plots for each foot movement mode recognition accuracy for the two strategies.

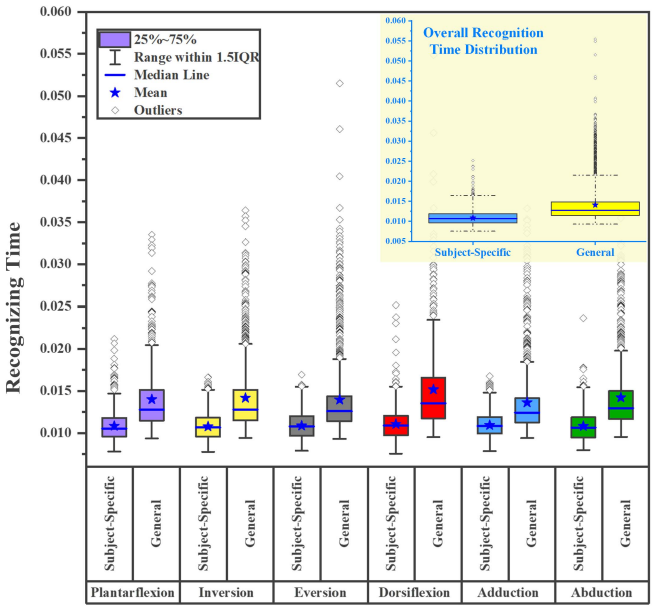

Fig. 13. Box plots for the prediction time analysis. The inside figure at the right corner shows for the overall prediction time comparisons of the two approaches of all subjects strides.

TABLE II
RECOGNITION TIME OF THE TEST RESULTS FROM THE TOTAL STRIDES OF ALL SUBJECTS

Unit: millisecond (ms)	Subject-Specific	General
Shortest Time	7.6	9.3
Longest Time	25.2	55.4
Average Time (mean)	10.9	14.1
Standard Deviation Time (SD)	1.7	4.5

We conducted another two one-tailed (lower tail) t-tests with a 99% confidence level ($(1-\alpha)\cdot 100\%, \alpha = 0.01$) to test the statistical significance of the system recognition time efficiency for two approaches separately. The one-tailed t-test often provides more power to detect an effect, which whether an approach influences the observing of our interests. We test against the alternative hypothesis that the recognition time population of the system steadily tends in one direction of effect less than 1.2 seconds [40], [42]. For the subject-specific approach, the simulated real-time recognition time of strides across all subjects varied from 7.6 to 25.2 ms (10.9 ± 1.7 ms, mean, and SD) ($p < 0.0001$). For the general approach, the recognition time varied from 9.3 to 55.4 ms (14.1 ± 4.5 ms, mean, and SD) for all subjects ($p < 0.0001$). Before the t-test, to check the normality assumption of the t-test, we conducted the normality test for the null hypothesis that both approaches system recognition time obeys normal distribution. Under the subject-specific approach, the system recognition time also accepts the null hypothesis ($p = 0.31$) and obeys normal distribution. Under the general approach, the system recognition time accepts the null hypothesis ($p = 0.12$) and also obeys normal distribution. The test statistic revealed that our proposed system has a high statistical significance for an adequate recognition time ($p < 0.0001$).

From the boxplot, Fig. 13 gives insight into the recognition time distribution. Similarly, we also performed a two-tailed

paired t-test with a 99% confidence level ($(1-\alpha)\cdot 100\%, \alpha = 0.01$) to test the statistical significance of the recognition time difference of our two approaches ($p = 0.0002$). The statistical inference community often used the two-tailed t-test to determine whether the interest groups of two approaches differ without specifying direction. The null hypothesis is that the recognition time population of the two approaches comes from the same distribution [42], [43]. The test statistic found a high statistical significance of the difference in recognition time of the two approaches ($p = 0.0002$).

IV. Discussion

The level and speed of an individual to adapt to the operation of a wearable device are strongly related to the control method of the HMI. Therefore, a supervisory mode recognition system's ability to respond to the user's motor intent determines the degree of optimal coordination and system efficiency. The study presented in this paper experimentally verified the feasibility of our proposed recognition system that captured the user's continuous multiple-DOF foot movements accounting for three degrees along three planes based on a solely kinematic signal source. In addition, the study experimentally compared the results of two approaches for guidance in future multiple-DOF wearable lower-limb rehabilitation robotics. It fills the demand for a recognition HMI control strategy of multiple-DOF wearable lower-limb rehabilitation robotics design, especially in AFOs.

A. System Analysis

Currently, no published studies have reported continuous three-DOF ankle-foot movement recognition, especially in HMI recognition control strategies for an AFO. The two existing studies on ankle-foot recognition [17], [19] both lack one DOF in the study, and neither calculates prediction time. Scott *et al.* study involves 2-DOF foot movement at approximately 86% recognition accuracy. The study lacks one DOF in the frontal plane also has no continuous locomotion recognition mode [19]. Gregory and Ren tried different strategies to recognize continuous multiaxial ankle-foot motions and yielded the highest intent prediction accuracy of 77.2%. The study only contains 2-DOF foot movements and lacks one DOF in the transverse plane (foot abduction and adduction) [17].

Our study has more DOFs with recognition of more foot movement modes during continuous locomotion. Meanwhile, our proposed system obtained better results in terms of accuracy [17], [19]. Additionally, compared with studies using a user's surface electromyography (sEMG) sensor [17], sEMG sensors rely on direct contact with human muscles to obtain stable and clear human muscle excitability; therefore, they are not suitable for individuals with limb insufficiency or limb pathology such as muscle atrophy. IMU signals can overcome these shortcomings.

As section III-A presents the raw signals of our proposed system, and our designed system's sensor position and signal source are validated to show the recognition potential. We applied a feature-selection technique and an algorithm to the normalized raw signal output from the designed system to further improve the system recognition effects. Specific features can capture the subtle difference of helpful information in dynamic signals and keep the model from being distracted by irrelevant information in the dynamic signals that will not impact recognition results. Our experimental results verified that the IMU dynamic signal combined with the algorithm and selected features through our system could effectively recognize continuous multiple-DOF foot movements. Compared with Gregory and Ren, who used six sEMGs in total, three sensors were placed on each leg [17]. Our proposed system has the advantage of convenience and practicality while also guaranteeing higher accuracy. Besides, our system gives out the calculation for the prediction time of each step than the previous study [17], [19]. The system can quickly perceive multiple degrees of freedom of the foot movement states during continuous locomotion. Our HMI multiple-DOF recognition system satisfies the high level of the control hierarchy in robot-assisted lower-limb devices. Users with our proposed system could control the devices more intuitively and efficiently. Our proposed system could also fill up the human ankle-foot motion monitoring demand. The system could assist the therapist, healthcare workers, and patients in diagnosis, treatment, and rehabilitation, such as gait abnormalities detecting, further observing pathological gaits for diagnosis, and robot-assisted home healthcare. Traditional methods are often limited by space and time. Coupled with our fully portable and wearable wireless system, the users get more choice and free themselves to address more aspects of their work and life.

B. Subject-Specific Approach vs. General Approach

As shown in the results of section III-B, the subject-specific approach maintains high stability and accuracy through recognition of all foot movement modes. The general approach has lower accuracy and relatively large fluctuations in a few foot movement modes, especially in recognizing the dorsiflexion mode. This confusing recognition may be caused by different individuals having unique movement habits. To summarize, the subject-specific approach yielded significantly better recognition results and was much more stable than the generic approach for all analyzed parameters.

As shown in the results of section III-C, we verified that the system responds quickly enough compared to an average adult stride time of 1.2 seconds under both approaches [39], [40]. We also found that the subject-specific model has a significantly shorter response time than the general model. We can see from Fig. 13 that there were no apparent trends or differences in the recognition of each foot movement mode. In summary, the system can provide a fast recognition response. The results also revealed that the recognition time has no significant trends for different foot movements. The subject-specific model can respond more quickly than the general model.

As discussed above, both our proposed general and subject-specific strategies are better than previous works [17], [19]. Our proposed system can recognize more DOFs containing more foot movements under a continuous locomotion

mode with a higher accuracy and calculate the prediction time for each step. We also evaluate the system performance of the two approaches under simulated real-time conditions. The experimental results show the high potential of the system using the subject-specific approach. The subject-specific model yielded better recognition performance for all analyzed parameters than the generic model. The reason behind this may be that individuals have different body physical conditions and unique foot movement habits. Our study results imply that choosing a subject-specific approach in future multiple-DOF lower-limb HMI rehabilitation device designs may be more effective.

C. Limitations

Our proposed system can recognize continuous multiple-DOF ankle-foot movements much more accurately than previous works [17], [19]. Although the accuracy is relatively decreased in the general model, this could be due to the differences in individual body physical conditions and movement habits. Overall, the significant results obtained with our proposed system provide further evidence that our systems can represent valid continuous multiple-DOF foot movement recognition.

Some design features of our system can be improved in the future. The accuracy of the general model still has room to improve. The subject-specific approach often implies a high cost. Generalizing the model can reduce industrial manufacturing costs. Although the general model is relatively less effective than the subject-specific model for each specific user, it still has considerable value. Since the general model can meet most users'general demands at a low cost, users can use it immediately for emergencies. If the user met conditions in the future, users could also choose a subject-specific model. Currently, this is a pilot study for validating the effectiveness of our proposed recognition wearable system for continuous multiple-DOF foot movements accounting for three degrees along three planes. In future work, we will primarily explore ways to increase the general approach recognition accuracy. In addition, it will be interesting to probe the system performance on different terrains. Another improvement we can make in the future is to reduce the number of sensors used rather than using two IMUs in each foot. Therefore, our future study will further simplify the system but maintain a high accuracy.

V. Conclusion

In this work, we first presented a proposal of an HMI recognition wearable system for continuous multiple-DOF foot movements accounting for three degrees along three planes. The experimental results of all subjects validated the system's effectiveness with satisfactory recognition accuracy and recognition time. Experimental results also demonstrated that the subject-specific approach outperformed the general approach in all analyzed evaluation results, including validity, reliability, and recognition time. Our study supplements the demands of multiple-DOF lower-limb rehabilitation robots, which are strongly related to the HMI control of AFOs and provides insights into future wearable rehabilitation device protocol designs in the foot and ankle.

Acknowledgment

The authors would like to thank the anonymous reviewers for their valuable suggestions, and also would like to thank Shichang Zhang for his help in fabricating and assembling the circuits and mechanical structures.

References

[1] R. Jiménez-Fabián and O. Verlinden, "Review of control algorithms for robotic ankle systems in lower-limb orthoses, prostheses, and exoskeletons," *Med. Eng. Phys.*, vol. 34, no. 4, pp. 397–408, May 2012.

[2] H. Herr, "Exoskeletons and orthoses: Classification, design challenges and future directions," *J. NeuroEng. Rehabil.*, vol. 6, p. 21, Jun. 2009.

[3] P. Cherelle, V. Grosu, A. Matthys, B. Vanderborght, and D. Lefeber, "Design and validation of the ankle mimicking prosthetic (AMP-) foot 2.0," *IEEE Trans. Neural Syst. Rehabil. Eng.*, vol. 22, no. 1, pp. 138–148, Jan. 2014.

[4] S. Viteckova, P. Kutilek, and M. Jirina, "Wearable lower limb robotics: A review," *Biocybern. Biomed. Eng.*, vol. 33, no. 2, pp. 96–105, 2013.

[5] W. Huo, S. Mohammed, J. C. Moreno, and Y. Amirat, "Lower limb wearable robots for assistance and rehabilitation: A state of the art," *IEEE Syst. J.*, vol. 10, no. 3, pp. 1068–1081, Sep. 2016.

[6] H. Fritz, D. Patzer, and S. S. Galen, "Robotic exoskeletons for reengaging in everyday activities: Promises, pitfalls, and opportunities," *Disability Rehabil.*, vol. 41, no. 5, pp. 560–563, Feb. 2019.

[7] A. K. Raj, P. D. Neuhaus, A. M. Moucheboeuf, J. H. Noorden, and D. V. Lecoutre, "Mina: A sensorimotor robotic orthosis for mobility assistance," *J. Robot.*, vol. 2011, pp. 1–8, Oct. 2011.

[8] W. Takano, J. Obara, and Y. Nakamura, "Action recognition from only somatosensory information using spectral learning in a hidden Markov model," *Robot. Auto. Syst.*, vol. 78, pp. 29–35, Apr. 2016.

[9] F. Gao, G. Liu, F. Liang, and W.-H. Liao, "IMU-based locomotion mode identification for transtibial prostheses, orthoses, and exoskeletons," *IEEE Trans. Neural Syst. Rehabil. Eng.*, vol. 28, no. 6, pp. 1334–1343, Jun. 2020.

[10] H. Huang, F. Zhang, L. J. Hargrove, Z. Dou, D. R. Rogers, and K. B. Englehart, "Continuous locomotion-mode identification for prosthetic legs based on neuromuscular–mechanical fusion," *IEEE Trans. Biomed. Eng.*, vol. 58, no. 10, pp. 2867–2875, Oct. 2011.

[11] T.-H. Hwang, J. Reh, A. O. Effenberg, and H. Blume, "Real-time gait analysis using a single head-worn inertial measurement unit," *IEEE Trans. Consum. Electron.*, vol. 64, no. 2, pp. 240–248, May 2018.

[12] J. Ryu, B.-H. Lee, J. Maeng, and D.-H. Kim, "SEMG-signal and IMU sensor-based gait sub-phase detection and prediction using a user-adaptive classifier," *Med. Eng. Phys.*, vol. 69, pp. 50–57, Jul. 2019.

[13] M. D. S. S. Manchola, M. J. P. P. Bernal, M. Munera, and C. A. Cifuentes, "Gait phase detection for lower-limb exoskeletons using foot motion data from a single inertial measurement unit in hemiparetic individuals," *Sensors*, vol. 19, no. 13, p. 2988, Jul. 2019.

[14] W. Huo, S. Mohammed, Y. Amirat, and K. Kong, "Fast gait mode detection and assistive torque control of an exoskeletal robotic orthosis for walking assistance," *IEEE Trans. Robot.*, vol. 34, no. 4, pp. 1035–1052, Aug. 2018.

[15] H. Kazerooni and R. Steger, "The Berkeley lower extremity exoskeleton," *J. Dyn. Syst. Meas. Control-Trans. ASME*, vol. 128, pp. 14–25, Mar. 2006.

[16] A. B. Zoss, H. Kazerooni, and A. Chu, "Biomechanical design of the Berkeley lower extremity exoskeleton (BLEEX)," *IEEE/ASME Trans. Mechatronics*, vol. 11, no. 2, pp. 128–138, Apr. 2006.

[17] U. Gregory and L. Ren, "Intent prediction of multi-axial ankle motion using limited EMG signals," *Frontiers Bioeng. Biotechnol.*, vol. 7, p. 335, Nov. 2019.

[18] S. Maragliulo, P. F. A. Lopes, L. B. Osorio, A. T. De Almeida, and M. Tavakoli, "Foot gesture recognition through dual channel wearable EMG system," *IEEE Sensors J.*, vol. 19, no. 22, pp. 10187–10197, Nov. 2019.

[19] J. Scott, D. Dearman, K. Yatani, and K. N. Truong, "Sensing foot gestures from the pocket," in *Proc. 23nd Annu. ACM Symp. User Interface Softw. Technol.*, 2010, pp. 199–208.

[20] J. A. de la Tejera, R. Bustamante-Bello, R. A. Ramirez-Mendoza, and J. Izquierdo-Reyes, "Systematic review of exoskeletons towards a general categorization model proposal," *Appl. Sci.*, vol. 11, no. 1, p. 76, Dec. 2020.

[21] A. J. Yoder, B. N. Mazzone, R. S. Miltenberger, and S. Farrokhi, "Biomechanical improvements following foot strike biofeedback training for a patient using a passive dynamic ankle-foot orthosis during running," *Prosthetics Orthotics Int.*, vol. 43, no. 4, pp. 447–452, 2019.

[22] C. Nikamp, J. V. D. Palen, H. Hermens, J. Rietman, and J. Buurke, "o28: A randomized controlled trial on providing ankle-foot orthoses in the early rehabilitation after stroke: The kinematic effects," *Gait Posture*, vol. 57, p. 50, Sep. 2017.

[23] H. Sankaranarayan, A. Gupta, M. Khanna, A. B. Taly, and K. Thennarasu, "Role of ankle foot orthosis in improving locomotion and functional recovery in patients with stroke: A prospective rehabilitation study," *J. Neurosci. Rural Pract.*, vol. 7, no. 4, p. 544, 2016.

[24] C. G. Pfeifer, S. Grechenig, B. Frankewycz, A. Ernstberger, M. Nerlich, and W. Krutsch, "Analysis of 213 currently used rehabilitation protocols in foot and ankle fractures," *Injury*, vol. 46, pp. S51–S57, Oct. 2015.

[25] S. Tyson, E. Sadeghi-Demneh, and C. Nester, "A systematic review and meta-analysis of the effect of an ankle-foot orthosis on gait biomechanics after stroke," *Clin. Rehabil.*, vol. 27, no. 10, pp. 879–891, Oct. 2013.

[26] K. A. Shorter, G. F. Kogler, E. Loth, W. K. Durfee, and E. T. Hsiao-Wecksler, "A portable powered ankle-foot orthosis for rehabilitation," *J. Rehabil. Res. Develop.*, vol. 48, no. 4, p. 459, 2011.

[27] S. Au, M. Berniker, and H. Herr, "Powered ankle-foot prosthesis to assist level-ground and stair-descent gaits," *Neural Netw.*, vol. 21, no. 4, pp. 654–666, May 2008.

[28] A. Gómez-Espinosa, N. Espinosa-Castillo, and B. Valdés-Aguirre, "Foot-mounted inertial measurement units-based device for ankle rehabilitation," *Appl. Sci.*, vol. 8, no. 11, p. 2032, Oct. 2018.

[29] R. W. Teasell, M. P. McRae, N. Foley, and A. Bhardwaj, "Physical and functional correlations of ankle-foot orthosis use in the rehabilitation of stroke patients," *Arch. Phys. Med. Rehabil.*, vol. 82, no. 8, pp. 1047–1049, Aug. 2001.

[30] L. Chinn and J. Hertel, "Rehabilitation of ankle and foot injuries in athletes," *Clinics Sports Med.*, vol. 29, no. 1, p. 157, 2010.

[31] M. Islam and E. T. Hsiao-Wecksler, "Detection of gait modes using an artificial neural network during walking with a powered ankle-foot orthosis," *J. Biophys.*, vol. 2016, pp. 1–9, Dec. 2016.

[32] P. K. Jamwal, S. Q. Xie, S. Hussain, and J. G. Parsons, "An adaptive wearable parallel robot for the treatment of ankle injuries," *IEEE/ASME Trans. Mechatronics*, vol. 19, no. 1, pp. 64–75, Feb. 2014.

[33] P. K. Jamwal, S. Hussain, and S. Q. Xie, "Three-stage design analysis and multicriteria optimization of a parallel ankle rehabilitation robot using genetic algorithm," *IEEE Trans. Autom. Sci. Eng.*, vol. 12, no. 4, pp. 1433–1446, Oct. 2015.

[34] P. K. Jamwal, S. Hussain, M. H. Ghayesh, and S. V. Rogozina, "Impedance control of an intrinsically compliant parallel ankle rehabilitation robot," *IEEE Trans. Ind. Electron.*, vol. 63, no. 6, pp. 3638–3647, Jun. 2016.

[35] J. A. Blaya and H. Herr, "Adaptive control of a variable-impedance ankle-foot orthosis to assist drop-foot gait," *IEEE Trans. Neural Syst. Rehabil. Eng.*, vol. 12, no. 1, pp. 24–31, Mar. 2004.

[36] C. L. Brockett and G. J. Chapman, "Biomechanics of the ankle," *Orthopaedics Trauma*, vol. 30, no. 3, pp. 232–238, 2016.

[37] E. L. Allwein, R. E. Schapire, and Y. Singer, "Reducing multiclass to binary: A unifying approach for margin classifiers," *J. Mach. Learn. Res.*, vol. 1, pp. 113–141, Sep. 2001.

[38] E. Alpaydin, *Introduction to Machine Learning*. Cambridge, MA, USA: MIT Press, 2020.

[39] R. B. Dale, "Principles of rehabilitation," in *Physical Rehabilitation of the Injured Athlete*. Philadelphia, PA, USA: Saunders, 2012, pp. 41–66.

[40] C. R. McAvoy *et al.*, "Cadence (steps/min) and relative intensity in 21 to 60-year-olds: The CADENCE-adults study," *Int. J. Behav. Nutrition Phys. Activity*, vol. 18, no. 1, pp. 1–15, Dec. 2021.

[41] R. O. Duda, P. E. Hart, and D. G. Stork, *Pattern Classification*, 2nd ed. Hoboken, NJ, USA: Wiley, 2012.

[42] G. Casella and R. L. Berger, *Statistical Inference*, 2nd ed. Boston, MA, USA: Cengage Learning, 2021.

[43] R. V. Hogg, M. Joseph, and T. C. Allen, *Introduction to Mathematical Statistics*, 6th ed. London, U.K.: Pearson, 2005.